

WPo4.9 – SIMULATION OF IFE CHAMBER DYNAMIC RESPONSE BY A SECOND ORDER GODUNOV METHOD WITH ARBITRARY GEOMETRY *

Zoran Dragojlovic and Farrokh Najmabadi

*Department of Electrical & Computer Engineering and Center for Energy Research
University of California in San Diego, 9500 Gilman Drive, La Jolla, CA 92093-0417*

ABSTRACT – *Many physical phenomena with different time scale occur in the chamber following the target explosion. After the target-generated X-rays and ion debris traverse the chamber, the chamber environment is in a non-equilibrium phase (e.g., non-uniform pressure) and material is introduced in the chamber (e.g., ejecta from the wall as well desorbed target constituents implanted in the wall). Afterward, the chamber environment evolves mainly in the hydrodynamics time scale. Understanding the evolution and dynamics of chamber environment at this “long” timescale is essential in developing a rap-rated laser-fusion facility. We have developed SPARTAN code to investigate chamber evolution. Strong shocks born out of the target blast are captured by a second order Godunov algorithm for compressible Navier-Stokes equations. Arbitrary chamber geometry is incorporated into a Cartesian grid and resolved by embedded boundary method. Simulation demonstrates the robustness of the numerical algorithm in treatment of highly nonlinear chamber dynamics with fast moving discontinuities. For this purpose, the effects of selected parameters (viscosity and heat conduction) on the chamber state prior to the insertion of the next target are estimated.*

I. INTRODUCTION

In a rep-rated laser-fusion facility, the pulse repetition rate is limited by the time it takes for chamber environment to return to a sufficiently quiescent and clean low-pressure state following a target explosion to allow a second shot to be initiated. Laser propagation and beam quality on the target as well target injection and tracking are impacted by the number density, temperature, and mix of chamber constituents as well as fluid eddies and turbulence in the chamber.

Many physical phenomena with different time scale occur in the chamber following the target explosion. The resultant X-rays, ion debris and neutron from the target travel through the chamber. Depending on the chamber constituents, X-rays and ion debris can interact and deposit part of their energy in the chamber, generating a shock wave that propagates through the chamber. The remaining portion of X-rays and ion debris arrive at the chamber wall. They interact and affect the surface wall materials in various ways that could result in the emission of atomic (vaporization) and macroscopic particles (such as graphite or carbon composites), thereby limiting the lifetime of the wall. This “first pass” of target X-rays and ion debris through the chamber can take up to a few microseconds. At the end of this phase, the chamber environment is in a non-equilibrium phase (e.g., non-uniform pressure) and a new source of material and is introduced in the chamber (e.g., ejecta from the wall as well desorbed H, He, and other target constituents

implanted in the wall).

After this “fast” timescale phase, the chamber environment evolves mainly in the hydrodynamics time scale and a new equilibrium condition is achieved after certain time interval. Understanding the evolution and dynamics of chamber environment at this “long” timescale is essential in developing a rap-rated laser-fusion facility.

It would be computationally prohibitive to develop a simulation code that can analyze chamber response in both fast and slow timescales as the relevant time scales, spatial scales, and underlying physics are vastly different. It would be much preferable to utilize a code suitable for fast time scale to estimate the evolution of the chamber environment for a few microsecond following target explosion. These results can then used by a simulation code suitable for “long” timescale which would follow the chamber environment for several hundred milliseconds.

The focus of our research effort is the development of a fully integrated computer code to model and study the chamber dynamic behavior in the “long” time scale, including: the hydrodynamics; the effects of various heat sources and transfer mechanisms such as photon and ion heat deposition and chamber gas conduction, convection, and radiation; the chamber wall response and lifetime; and the cavity clearing. Since developing such a simulation capability is a major undertaking, the development of the code is envisioned in several steps of increasing sophistication. In

*Research was supported by naval Research’s Laboratory under grant N00173-02-1-6010.

this paper, we report on our initial results from SPARTAN code.

At present, SPARTAN solves 2-D transient compressible Navier Stokes equations. Code is written in a modular fashion so that extrapolation to 3-D geometry is straight-forward. Behavior of strong shocks born out of the target blast are captured accurately by a second order Godunov algorithm. Diffusive terms (viscosity and thermal conductivity) are included and can depend on state variables (*e.g.*, local temperature). Uniform accuracy throughout the fluid domain is obtained by adaptive mesh refinement. This is essential as the width of shock region is usually several orders of magnitude smaller than the chamber dimensions. Arbitrary chamber geometry is incorporated into a Cartesian grid and resolved by embedded boundary method. Simulation results demonstrates the robustness of SPARTAN numerical algorithms in studying highly nonlinear chamber dynamics with fast moving discontinuities.

In this paper, we will first provide a short summary of numerical algorithms in SPARTAN (Sec. 2). In Sec. 3 we present several simulations to show the capabilities of SPARTAN. For this purpose, we have studied the impact of selected parameters (viscosity and the conductive heat transfer across the wall) on the chamber state prior to the insertion of the next target. Conclusions and future plans for SPARTAN are discussed in Sec. 4.

II. NUMERICAL METHOD

Most state-of-the-art computational fluid dynamics codes use a variant of CGF algorithm [1] that is based on a second-order Godunov scheme and is suitable for modeling strong shocks and multi-fluid systems. In SPARTAN, the compressible Navier-Stokes equations are discretized using a finite-volume method. The numerical integration is performed by a variant of CGF method that is suitable for solving problems with irregular geometry on Cartesian grids was developed by Pember *et al.* [2]. The time-centered conservative fluxes are computed at the geometric center of full cell edges in the domain based on a Taylor-series extrapolation in space and time of the governing equations. States extrapolated from each of the two sides of an edge constitute the left and right states of a generalized Riemann problem. The Riemann problem is resolved with an approximate solver to obtain a single edge state for use in computing conservation fluxes into each cell. For cells where the edge is only partially inside the valid domain, fluxes values are interpolated from full-edge centers to the midpoint of the partial edge. The divergence of these conservation fluxes may

then be used to update the state, however the resulting increment may be numerically unstable for arbitrarily small partial cells. A stable and consistent, but non-conservative update is formed to update such cells, and conservation is instead enforced by local redistribution to the local neighborhood of such cells.

In order to obtain uniform accuracy over the solution domain, it is necessary to use high density grid around the moving structures such as shock waves and eddies, while using the low density grid elsewhere. This is possible by implementing the adaptive mesh refinement algorithm (AMR), as demonstrated in Refs. [2, 3]. SPARTAN's adaptive mesh refinement algorithm organizes the computational grid into levels which vary in grid density from coarse to fine. The fluid domain is defined on the coarsest level grid. A tagging algorithm runs on this level at every time step and tags all the cells which have a high difference in density or energy across them. Higher level grids are placed over the tagged cells, then the tagging algorithm runs again until either the highest grid level is reached or the refinement criteria are satisfied. The grid is refined at every time step as the solution rapidly changes.

Details of numerical methods utilized in SPARTAN and convergence and accuracy tests are given in Ref. [4].

III. RESULTS AND DISCUSSION

We have simulated the dynamic evolution of a laser-IFE chamber. The chamber radius is 6.5 m. A 20-m long laser beam line with a diameter of 1 m is also included to study the impact of blast shock waves on the final optics. The chamber was filled with Xe gas at a pressure of 6.67 Pa (50 mTorr) at room temperature. The direct-drive target [5] has a yield of 160 MJ. Target explosion is modeled by the 1-D Lagrangian code BUCKY [6]. The target X-ray and ions heat the Xe gas which is subsequently cooled through radiation. The chamber state at 500 μ s was estimated. At this point in time, the Xe gas in the chamber has cooled down to about 2 eV and radiation losses has become negligible. At the same time, the shock wave from target explosion has not yet reached the chamber wall, and therefore, 1-D results from Bucky can be interpolated for analysis with a higher-dimension code such as SPARTAN.

Bucky's results [7] have been used as the initial condition for SPARTAN. The initial condition was interpolated onto the 2-D grid by rotation of the 1-D BUCKY solution about the blast location, as is shown in Fig. 1. For simulations reported here, SPARTAN is exercised with a single species, *i.e.*, chamber Xe gas. The chamber gas is represented by an ideal

equation of state. The viscosity and thermal conductivity are dependent on temperature. The boundary conditions on the wall included zero mass flux, reflective velocity and the energy flux that was either zero or determined by heat conduction from the fluid to the wall. In the latter case, the wall was kept at the constant temperature of 700°C.

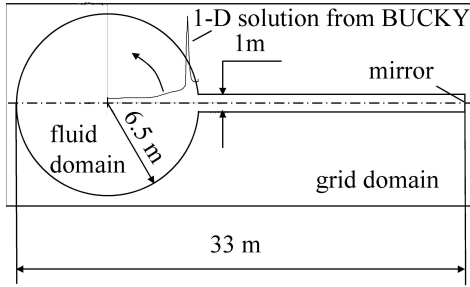


Figure 1: Fig. 1. Geometry and initial conditions for the cylindrical chamber with a laser beam channel on the side.

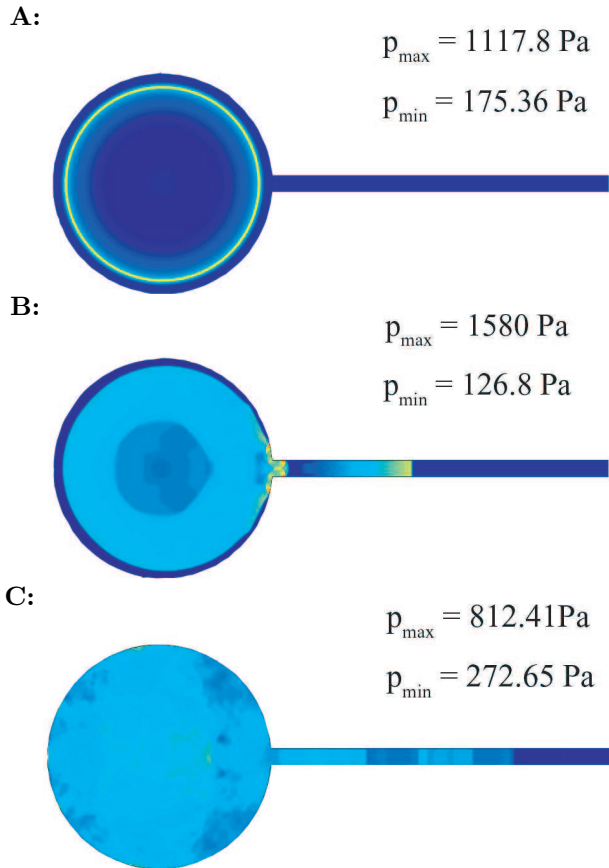


Figure 2: Contours of pressures in the chamber for Case I at A) $t = 500 \mu\text{s}$ (start of SPARTAN simulation), B) at $t = 5.0\text{ms}$ (the shock wave has traveled through the chamber once), C) at $t = 50 \text{ms}$.

Three different cases are considered. Case I: viscosity and heat conduction of the chamber gas were set to zero, the target blast was set in the center of the chamber and the wall was thermally insulated. This case represents the point of departure to study the impact of diffusive processes on the chamber evolution. Case II: Gas heat conductivity has been included (no viscosity) to simulate the “cool-down” of the chamber gas. Case III: Gas viscosity is included (but no conduction) to investigate the impact of viscosity to damp out the gas velocity and pressure fluctuations and eddies in the chamber.

Figure 2 presents pressure contours in the chamber for Case I. Figure 2A is the start of SPARTAN simulation and the shock wave has not reached the chamber wall. In Fig. 2B ($t = 5.0\text{ms}$) the shock has been reflected and traveled through the chamber once. The initial and the secondary shocks can be clearly seen in the laser beam channel. In Fig. 2C ($t = 50\text{ms}$), the shock has bounced in the chamber 10 times and flow mixing has led to a reduction of peak velocities and pressure. The evolution of chamber is quite slow after this time. For example, at ($t = 100\text{ms}$), the peak pressure in the chamber is reduced to 760 Pa compared to 812 Pa at $t = 50\text{ms}$.

Figure 3A shows the temporal profile of pressure at the chamber wall with each peak denoting the reflection of the shock wave from the chamber wall. It can be seen that the shock wave dissipates rapidly. The pressure forces on the wall as well as the induced mechanical stresses are quite small. Figure 3B shows the temporal profile of pressure at the final optics location. Because the laser beam channel is 20 m long, the shock in the chamber bounces twice before the first shock wave reaches the final optics. After that time, the shock waves from the chamber moving toward the final optics and reflected shock waves from the final optics moving toward the chamber interact with each other. This leads to a drop in the pressure at the final optics location at $t \approx 0.06 \text{ms}$. It can also be seen that the pressure forces on the final optics location are quite small (Here we have assumed that the final optics are perpendicular to the laser beam channel. For grazing incident mirror, the pressure forces will be smaller by an order of magnitude.)

Figure 4 shows the temperature of the Xe gas in the center of the chamber. After the first reflection from the wall, the shock converges in the chamber center, heating a central core (about 20% of the chamber radius) to a much higher temperature (around 40 eV). This region “cools” down in a long time scale (10s of ms) through mixing. The individual peaks in temperature profile seen in Fig. 4 is the changes in temperature in a localized point. On average, the heated

central core size and temperature reduce smoothly in this time interval.

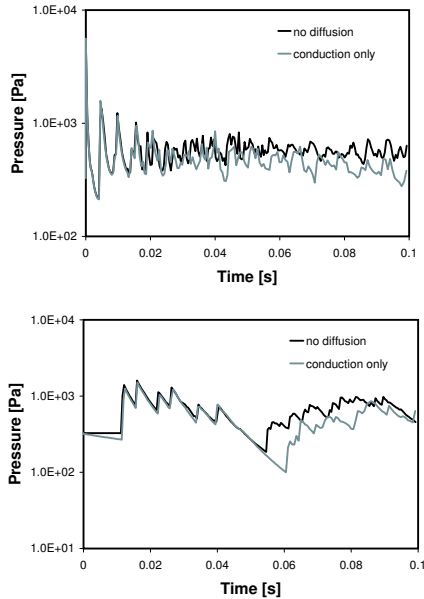


Figure 3: The pressure history on A) the chamber wall, and B) location of the final optic for cases I and II.

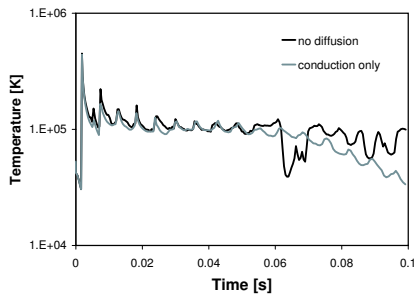


Figure 4: The temperature history at the center of the chamber for cases I and II.

Gas Conductivity: Figs. 3 and 4 also show the impact of gas conductivity on the chamber cool down. During the first 50 ms, the central hot core shrinks in size and vanishes (see Fig. 4). As such, the central temperature is not decreasing. After that time, the chamber gas cools down more or less uniformly. It is obvious that it would take tens of second before the chamber gas reaches an equilibrium with the chamber of wall (700°C) which was the initial condition taken by the Bucky code. Several iteration between Bucky and SPARTAN is needed to find the equilibrium chamber conditions prior to initiation of target explosion.

Gas Viscosity: Our simulations of Case III (including viscosity but no conduction) shows that viscosity generates large eddies in the chamber and average chamber temperature is increased by $\sim 20\%$ compared

to Case I. Because of the log scale in Figs. 3 and 4, Case III results are similar in size and nature to Case I and are not plotted.

III. DISCUSSION

SPARTAN simulation of target explosion in a laser-IFE chamber shows:

- 1) Two-dimensional affects are critical in assessing chamber dynamics.
- 2) Both gas conductivity and viscosity impact the chamber environment.
- 3) Gas conductivity is not sufficient to cool down the chamber to equilibrium with the chamber wall in between shots (~ 100 ms) as previously envisioned.
- 4) A hot central region is formed after the convergence of reflected shock in the chamber center. As a result, there exist a background plasma in the chamber. Radiation from and electron heat conduction of this plasma can cool down the chamber in a much more rapid manner. It is essential to include this background plasma in the simulations, a feature that will be shortly implemented in SPARTAN.

5) Viscous effects generate eddies in the chamber. However, viscosity of neutral gas is insufficient to damp out these eddies in the time between shots. These eddies may impact the target trajectory during the injection into the chamber. Since the laser beam channel geometry has a major impact on the initiation of these eddies, the larger number of beam channel in a laser-IFE facility will lead to more numerous but smaller eddies that may be damped out more readily. In addition, cool down of the chamber background due to the presence of background gas can help in reducing the size of these eddies.

References

- [1] H. M. Glaz, P. Colella, J. P. Collins, and R. E. Ferguson, *AIAA Journal*, pp 26-705, 1987.
- [2] R. B. Pember, J. B. Bell, P. Colella, *et. al*, *J. Comp. Phys.*, **120:2**, pp. 278-304, 1995.
- [3] A. S. Almgren, J. B. Bell, P. Colella, *et. al*, *J. Comp. Phys.*, **142**, pp. 1-46, 1998.
- [4] Z. Dragojlovic, F. Najmabadi, and M. Day, "Submitted to *J. Comp. Phys.*,
- [5] S. E. Bodner, D. G. Colombant, A. J. Schmitt and M. Klapisch, *Phys. of Plasmas*, **7**, pp. 2298-2301, 2000.
- [6] J. J. MacFarlane, G. A. Moses, R. R. Peterson, University of Wisconsin, Fusion Technology Institute report UWFD-984, 1995.
- [7] D. Haynes, University of Wisconsin, Madison, private communications.